OBSERVATIONS OF THE MARS POLAR VORTEX. T. H. McConnochie[1], B. J. Conrath[1], P. J. Gierasch[1], D. Banfield[1], M. D. Smith[2], [1]Dept. of Astronomy, Cornell University, Ithaca, NY 14853 (mcconnoc@astro.cornell.edu), [2]Goddard Space Flight Center.

Introduction: The winter season, westerly circumpolar flow of the Martian atmosphere, and of the terrestrial stratosphere, is concentrated into a jet whose latitude falls between 60 and 80 degrees. This jet is known as the polar vortex. The terrestrial polar vortex has been understood to be the dynamical controlling mechanism for ozone depletion in the polar stratosphere [e.g., 1] for more than a decade. More recently, the earth's stratospheric annular modes, which are essentially a weakening/strengthening oscillation of the polar vortex jet, have been shown to be coupled to and possibly even a driving mechanism for, the tropospheric Arctic Oscillation (AO) / North Atlantic Oscillation (NAO) phenomenon [2]. The AO / NAO is a key player in northern temperate zone winter weather patterns [3] and an increasing bias towards the positive (stronger polar vortex) phase in the past 30 years has been shown to be correlated with global warming trends [4].

The Martian polar vortex is important not only as an analog to the terrestrial vortex, but as a possible controlling factor in key Mars climate processes. For example, just as the terrestrial polar vortex chemically isolates the polar stratosphere, the Martian polar vortex may act as a barrier to the transport of dust and ice aerosols towards the winter pole, thus influencing the water cycle and affecting the composition of the seasonal polar cap.

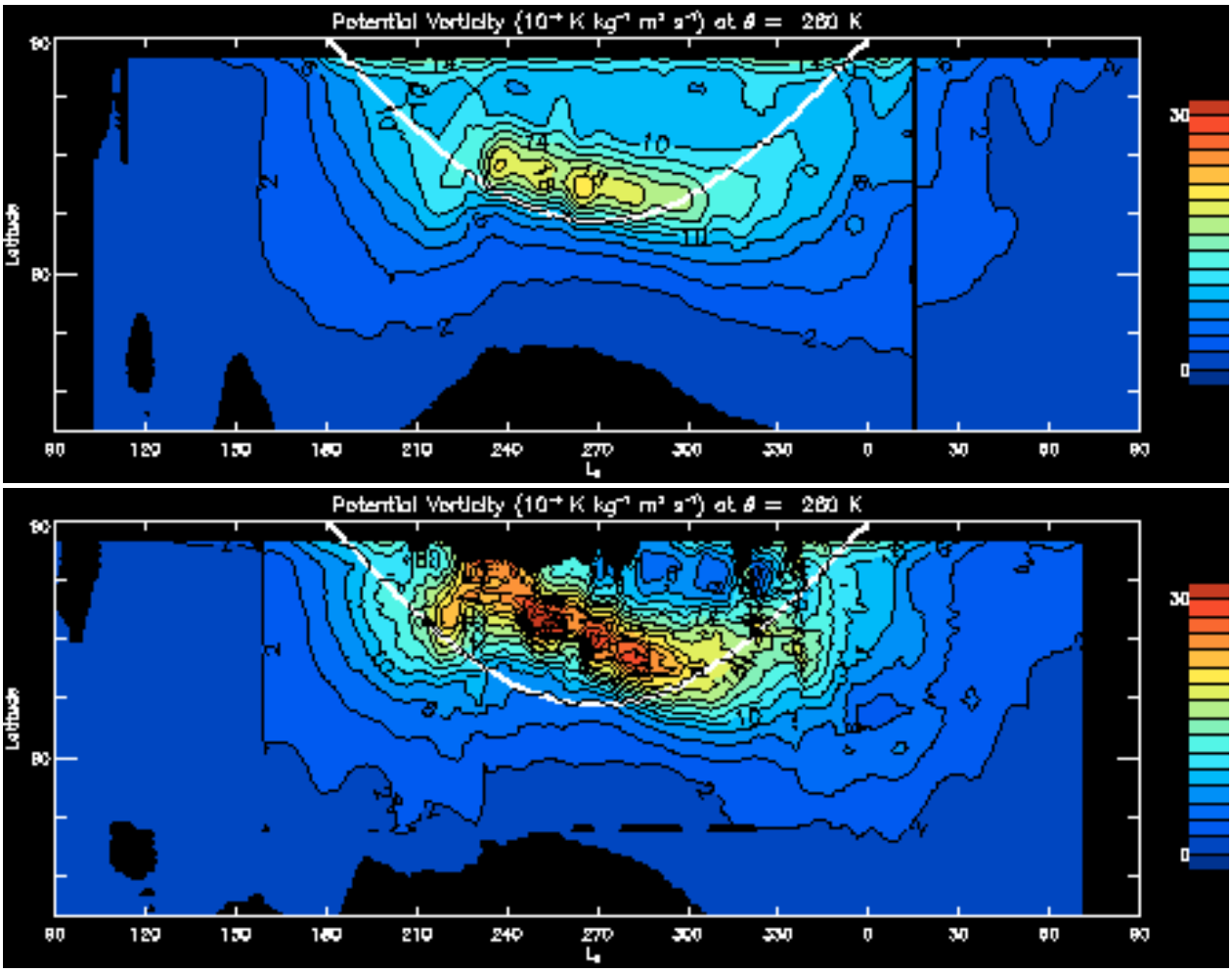

Figure 1: Potential vorticity on an isentropic surface versus latitude and time for MGS mapping years 1 (top) and 2 (bottom).

Method: We study the polar vortex structure both in the zonal mean sense (e.g., Figure 1) and in a longitudinally resolved sense (e.g., Figure 2). In order to do so, we use two types of data structures. In both cases, we vertically sample the temperature field uniformly in log-pressure coordinates at one-half scale height intervals. For the zonal mean, we bin the temperatures in one-degree bins of L_s and in one-degree bins of latitude. For the results presented here, the zonal mean temperatures have been smoothed in L_s with a 7-degree boxcar average. For the longitudinally resolved case, we generate a uniform, four-dimensional grid, in longitude, latitude, log-pressure, and time coordinates. The results presented here have a sampling interval of one degree in latitude, 10 degrees in longitude, and one sol in time. Once our 4-D and zonal-mean data structures are in hand we generate derived quantities such as the geopotential height, the horizontal wind field, and Ertel potential vorticity. For analysis, we usually chose to interpolate these quantities onto an isentropic vertical coordinate system.

Our temperature data come from the Mars Global Surveyor Thermal Emission Spectrometer (MGS-TES) temperature retrievals [5]. To date we have considered only nadir-pointed retrievals. We have also incorporated the MGS-TES column-integrated dust and ice aerosol retrievals [6,7] into our longitudinally resolved data structure. MGS is in a 2pm / 2am sun-synchronous polar orbit. MGS ground tracks are separate by approximately 30 degrees in longitude and 2 hours in time at a given latitude. To date we have considered only the daytime temperature data.

Our gridding procedure smoothes and resamples data points along the ground track, and then performs a bilinear interpolation in longitude and time. We then vertically integrate the temperature field to derive geopotential height. The temperature and geopotential height data are then gaussian smoothed to further reduce noise in the data set prior to calculating other derived quantities. The results presented here use gaussians with 50 degrees full-width-half-maximum (FWHM) in longitude and 5 degrees FWHM in latitude. We derive our horizontal wind field using the "balance winds" method suggested by Randel [8]. The "balance winds" method converges iteratively to a wind solution using the full horizontal momentum balance equations, neglecting only the vertical wind component and the Eulerian time derivatives. It is then straightforward to calculate Ertel potential vorticity from the wind field.

Results:. Figures 1 and 2 show Ertel potential vorticity on isentropic (i.e., constant potential temperature, θ) surfaces in the zonal mean and in a longitudinally resolved time series, respectively. For adia-

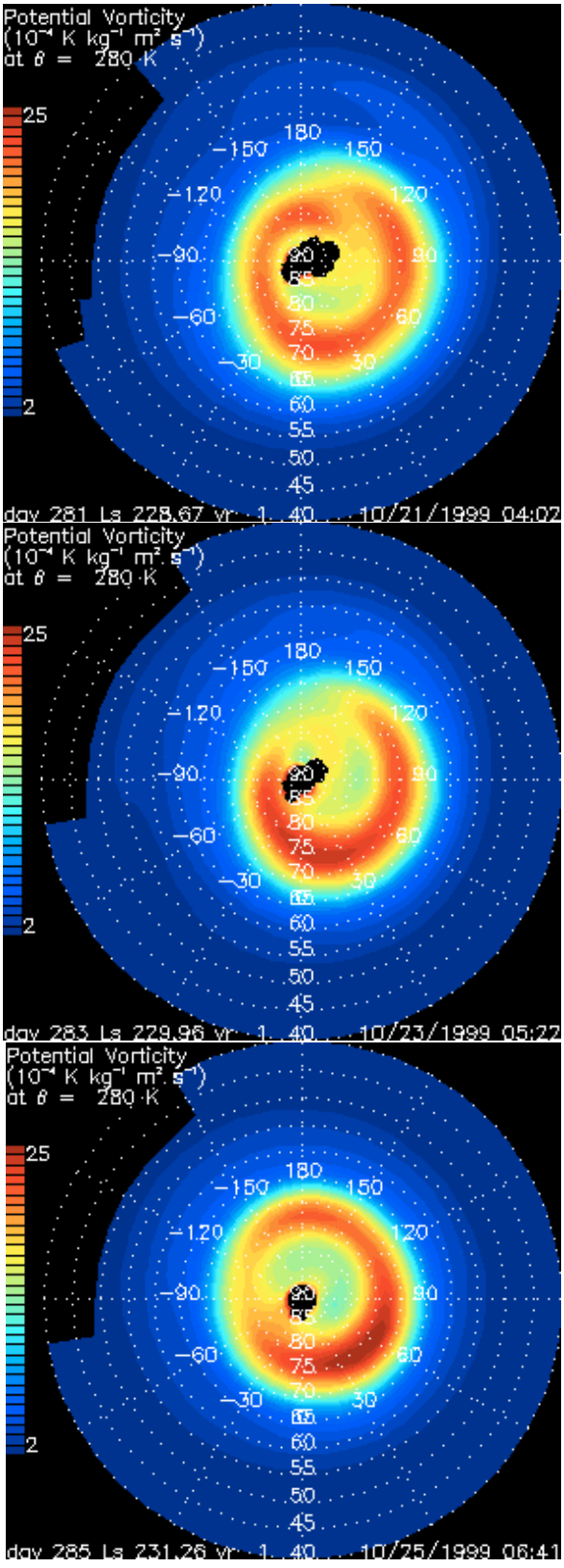

Figure 2: Time series of Ertel potential vorticity on an isentropic surface

batic flow, potential vorticity and entropy are both conserved following the motion. Therefore, to the extent that diabatic processes are negligible, and to within the accuracy of our wind solution, the potential vorticity contours on maps such as Figure 2 are streamlines.

In Figure 1, the bottom panel shows the year of the global dust storm. We can see that the zone of high potential vorticity that characterizes the polar vortex is, in the global-dust-storm year, displaced northwards and intensified in the early winter as compared to the same season of the preceding year.

Figure 2 shows a time series of the most striking polar vortex event in the first (global-dust-storm-free) mapping year. The normally annular zone of high PV is broken into a spiral shape for a period of approximately three days. This event corresponds with the early winter onset of regional dust storm activity.

The high-potential-vorticity (PV) zone of the polar vortex is normally annular in shape. The global dust storm period in Figure 1 is an apparent exception to this, with PV possibly increasing monotonically all of the way to the pole during the early winter of the dust storm year. The terrestrial polar vortex never shows an annular PV field, and normally PV increases monotonically towards the pole [e.g., 9].

Figure 3 presents a different approach to analysis of the MGS-TES dataset for polar vortex properties. It shows the first four principal components of the temperature field at a single pressure level during the northern winter of the first mapping year. Principal component 1 is primarily the linear time trend in polar temperatures. Principal components 2 and 3 represent a combination of stationary and traveling zonal wave-

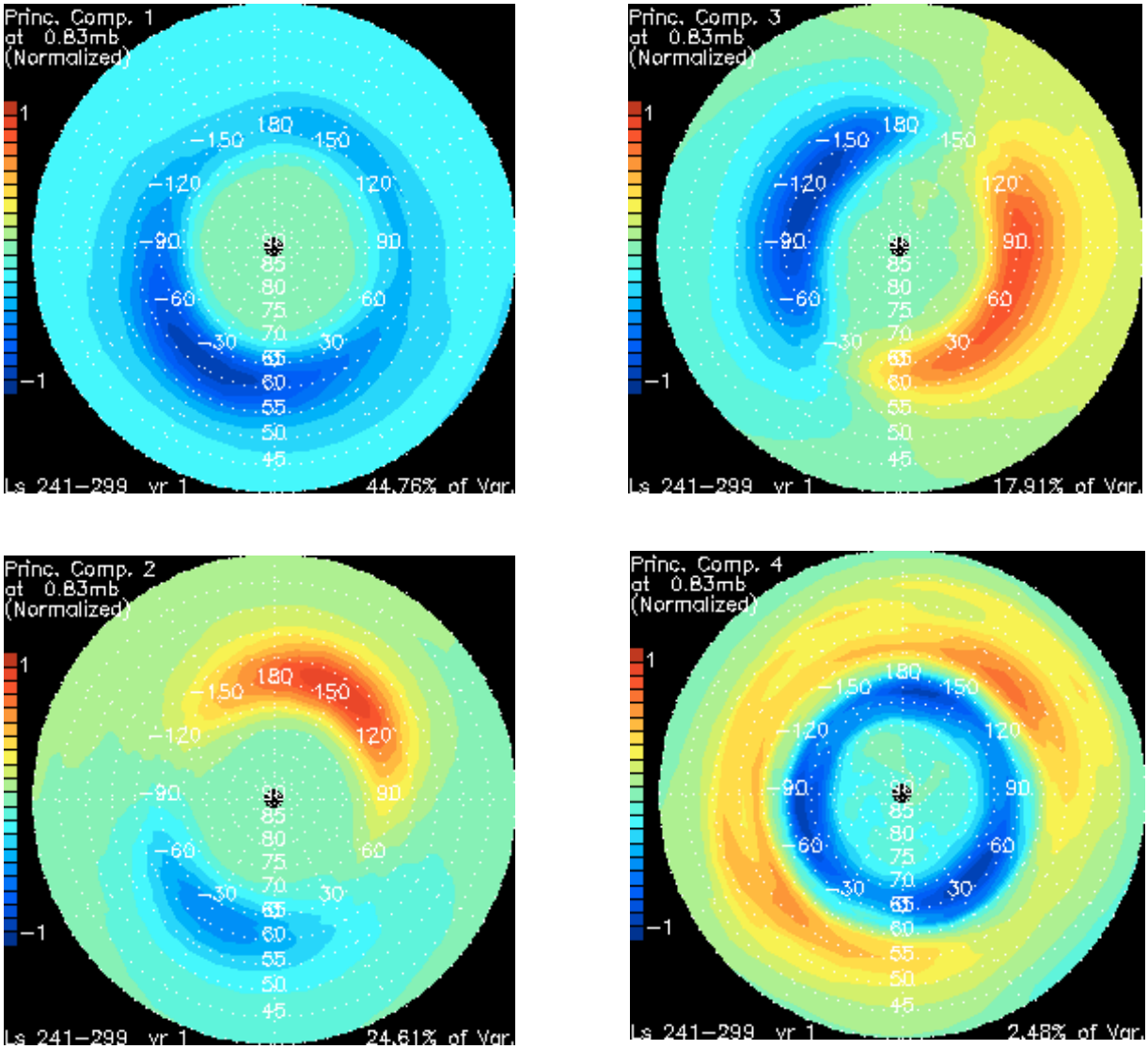

Figure 1: Principal Components of temperature variability on a pressure surface for mid-winter in the northern hemisphere of Mars

number 1 planetary waves, consistent with the fourier analysis of Banfield et al. [10]. Principal component 4 is an annular mode which may be analogous to the annular modes of the terrestrial stratosphere and/or the terrestrial Arctic Oscillation / North Atlantic Oscillllation (AO / NAO).

References: [1] Schoeberl M. R. and Hartmann D. L. (1991) *Science, 251,* 46. [2] Baldwin M. P. and Dunkerton J. D. (2001) *Science, 294,* 581. [3] Thompson D. W. J. and Wallace J. M. (2000) *J. Climate, 15,* 1000. [4] Thompson D. W. J. *et. al*. (2000) *J. Climate, 15,* 1018. [5] Conrath B J. *et. al.* (2000) *JGR, 105*, E4 9,509, [6] Smith, M. D. *et. al.* (2000) *JGR, 105*, E4 9,539. [7] Pearl, J. C. *et al.* (2001) *JGR, 106I, 12,325*, [8] Randel, W. J. (1987) *J. Atmos. Sci., 441,* 3097, [9] Nash, R. N., *et. al.* (1996) *JGR, 101*, D5 9,471. [10] Banfield D. B. *et. al.* (2003) *Icarus, 161*, 319.